

# Orientalional Dynamics of Liquids Confined in Nanoporous Sol–Gel Glasses Studied by Optical Kerr Effect Spectroscopy

RICHARD A. FARRER AND JOHN T. FOURKAS\*

*Eugene F. Merkert Chemistry Center, Boston College, Chestnut Hill, Massachusetts 02467*

Received January 16, 2003

## ABSTRACT

When a liquid is restricted to volumes on a molecular distance scale, its orientational and translational dynamics are perturbed strongly by the confinement. Nanoporous sol–gel glasses are an excellent model system for studying the effects of confinement on the behavior of liquids, and in this Account we review experiments in which ultrafast optical Kerr effect spectroscopy has been used to study the orientational dynamics of liquids confined in these media. We contrast the effects of confinement on the orientational dynamics of weakly wetting, strongly wetting, and networked liquids, and we discuss the influence of factors such as pore size, molecular shape, and surface chemistry.

## Introduction

Confinement of a liquid on a distance scale on the order of a few molecular diameters has a strong influence on its structure and dynamics. Beyond the intrinsic interest in understanding how finite-size effects influence liquids, confined liquids play an important role in fields such as catalysis, lubrication, separations, oil recovery, cellular dynamics, and microfluidic technology. As a result, the structural and dynamic properties of liquids confined in small spaces have received considerable attention in recent years.<sup>1,2</sup>

There are several mechanisms through which confinement affects the behavior of liquids. For instance, attractive interactions with confining surfaces can play a major role in inhibiting the dynamics of molecules. As the volume of the confining region decreases, the fraction of liquid molecules in contact with the surfaces increases. Thus, even liquids that have weak attractions to the surfaces are affected significantly by confinement. The shape of the liquid molecules and the interactions among them also play important roles in influencing the behavior of confined liquids.

Monitoring the dynamics of liquids confined to small volumes is a challenge in itself. When studying confined

liquids, one must ensure that changes in dynamics induced by the surfaces are detectable over the dynamics of the bulk liquid. Solving this problem requires either a system in which a large fraction of the liquid molecules are in contact with the surfaces or a technique that probes interfacial dynamics selectively. Since the chemical nature of the confining surfaces may additionally be important, using a system in which this property can be modified also has distinct advantages.

In 1986, Warnock, Awschalom, and Schafer<sup>3</sup> reported the first time-resolved study of the dynamics of liquids confined in nanoporous sol–gel glasses.<sup>4</sup> Using optical Kerr effect (OKE) spectroscopy,<sup>5,6</sup> they found that the orientational diffusion time of confined CS<sub>2</sub> was identical to that of the bulk liquid. However, the OKE signal for nitrobenzene confined to glasses having hydrophilic surfaces decayed on two separate time scales, one of which was similar to that of the bulk liquid and the other of which was approximately three times slower. When the same experiment was performed in hydrophobic pores, the decay rate of the OKE signal matched that in the bulk liquid. It was thus concluded that the reorientational retardation observed in confinement arose from interactions with the surface hydroxyl groups of the glasses.<sup>3</sup>

Since this initial work, many techniques have been employed to probe the dynamics of liquids confined in sol–gel glasses, including Raman spectroscopy,<sup>7–9</sup> NMR,<sup>10–14</sup> Rayleigh-wing scattering,<sup>15–17</sup> time-resolved phosphorescence<sup>18–20</sup> and fluorescence spectroscopies,<sup>21</sup> and dielectric spectroscopy.<sup>22–26</sup> Of particular relevance here are the studies of Jonas and co-workers, who have employed NMR<sup>10–14</sup> and Raman<sup>8,9</sup> spectroscopies to gain detailed insights into the orientational dynamics of liquids confined in sol–gel glasses. For instance, while Warnock et al. did not have the experimental sensitivity to discern a difference between the dynamics of bulk and confined CS<sub>2</sub>,<sup>3</sup> Jonas and co-workers were able to determine that CS<sub>2</sub> near pore surfaces has dynamics that are retarded as compared to those of the bulk.<sup>9,14</sup>

Here we recount the results of experiments in which we have used ultrafast OKE spectroscopy to study the dynamics of liquids confined in nanoporous sol–gel glasses. Silicate sol–gel glasses<sup>4</sup> are excellent media in which to study confined liquids. The high optical quality and low birefringence of these materials help to keep background signal to a minimum. By varying the synthetic conditions, the pore diameter can be varied between 15 and 100 Å, with a small standard deviation. The surfaces of the pores feature silanol groups, which render the glasses hydrophilic. The chemistry of these silanol groups is well-known, allowing the chemical nature of the pore surfaces to be modified with a variety of organosilane reagents.<sup>27</sup>

Advances in laser technology allow us to obtain OKE data with a signal-to-noise ratio that is orders of magnitude larger than was possible when this technique was

Richard A. Farrer was born in Grand Rapids, MI, in 1968. He received his BS from Aquinas College, MI, in 1991 and his PhD from Boston College in 2001. He is currently a postdoctoral fellow at Boston College involved in research ranging from ultrafast spectroscopy to nanoparticles and microfabrication.

John T. Fourkas was born in 1964 in Alameda, CA. He received his BS and MS in chemistry from Caltech in 1986, and his PhD in chemistry from Stanford in 1991. After spending time as a postdoctoral fellow at the University of Texas at Austin and MIT, in 1994 he joined the faculty of Boston College, where he is a professor of chemistry. His research interests include ultrafast dynamics of liquids and applications of multiphoton microscopy and fabrication.

\* Corresponding author.

first used to study confined liquids.<sup>3</sup> OKE spectroscopy allows us to obtain detailed, quantitative information about the structure and dynamics of liquids confined in sol–gel glasses. The information obtained is complementary to that provided by NMR and Raman spectroscopies, in that OKE spectroscopy measures the collective orientational correlation function of a liquid as opposed to the single-molecule orientational correlation function.<sup>28,29</sup> Below we demonstrate that OKE spectroscopy can reveal how confinement affects the orientational dynamics of weakly wetting, strongly wetting, and networked liquids, as well as how these dynamics are influenced by factors such as pore size, the composition of the pore surfaces, and the shape of the liquid molecules.

## Experimental Methods and Materials

Our experimental apparatus employs a Ti:sapphire laser that produces 50 fs pulses with a center wavelength of 800 nm at a repetition rate of 76 MHz. The apparatus has been described in detail elsewhere,<sup>30</sup> so here we provide only a brief description of the operating principles of OKE spectroscopy.<sup>30–32</sup> When a transparent liquid composed of anisotropically polarizable molecules is exposed to an intense ultrafast laser pulse (the “pump”), a dipole moment is induced along the axis of maximum polarizability of each molecule. The pump pulse serves as a “starting gun” for molecular dynamics by coherently exciting the Raman-active low-frequency and orientational modes of the liquid, including frustrated oscillatory motions (librations). Coherent librational motion damps out over a few picoseconds, leaving a slight orientational anisotropy in the liquid. The intrinsic orientational diffusion of the liquid molecules causes this induced order to decay on a time scale of picoseconds or longer.

The orientational anisotropy induced by the pump pulse creates a slight birefringence in the liquid. To determine the net molecular alignment in the sample, a low-intensity “probe” pulse that is polarized at 45° with respect to the pump pulse is passed through the sample and into a perpendicular “analyzer” polarizer. If no birefringence is encountered, none of the probe pulse passes through the analyzer. However, if the probe pulse encounters birefringence within the sample, its polarization will be modified, and a portion will pass through the analyzer. By varying the arrival time of the probe pulse, the birefringence of the liquid can be probed before, during, and after the pump pulse, thereby measuring the buildup and decay of the orientational anisotropy. We typically obtain scans out to delay times of a few tens of picoseconds to 100 ps, depending on the rate at which the anisotropy in the liquid relaxes.

We synthesize sol–gel glass samples using a two-step acid/base catalyzed procedure developed by Brinker that produces samples containing tortuous cylindrical pores that occupy roughly half of the volume of a monolithic sample.<sup>4</sup> Prior to use, the cylindrical samples are sanded to a thickness of approximately two millimeters, after which both sides are polished to optical quality.

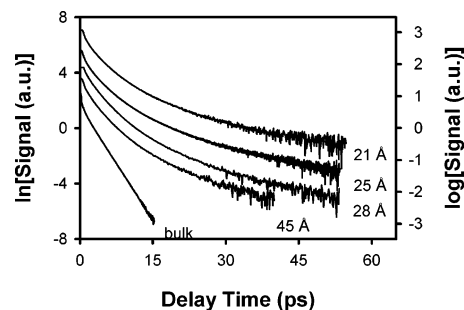


FIGURE 1. Representative CS<sub>2</sub> OKE decays obtained at 290 K. The data sets have been displaced for clarity.<sup>34</sup>

## Weakly Wetting Liquids

By virtue of their modest attractive interactions with pore surfaces, weakly wetting liquids are well suited for studying the role of physical features, such as molecular shape and pore size, in the behavior of confined liquids. A prototypical weakly wetting liquid that gives a strong OKE signal is CS<sub>2</sub>.<sup>33,34</sup> Figure 1 displays room-temperature OKE decays of CS<sub>2</sub> in the bulk and confined in 21, 25, 28, and 45 Å diameter pores.<sup>34</sup> At times less than 5 ps, librational dynamics account for a significant portion of the OKE signal. We will focus on longer times, for which the decay is dominated by reorientational dynamics. As is expected for a liquid composed of linear molecules, the reorientational dynamics of bulk CS<sub>2</sub> can be described by a single-exponential decay,<sup>28</sup> the time constant of which we denote  $\tau_{\text{bulk}}$ . However, the dynamics of the nanoconfined liquid exhibit a pore-size-dependent decay that is significantly slower than that of the bulk liquid.<sup>34</sup>

The OKE decays for the confined liquid can be fit empirically by a sum of three exponentials.<sup>34</sup> The time constant of the fastest exponential is always similar to that of the bulk liquid, and so it was constrained to equal  $\tau_{\text{bulk}}$ . This portion of the decay arises from molecules that are far enough from the pore walls that their orientational dynamics are unaffected by confinement. The remainder of the decay arises from molecules having dynamics that are inhibited by proximity to the pore surfaces. The intermediate time constant,  $\tau_2$ , is 3–4 times larger than the  $\tau_{\text{bulk}}$ , while the longest time constant,  $\tau_3$ , is 3–5 times larger than  $\tau_2$ . Thus, even though CS<sub>2</sub> has only weak attractive interactions with the pore walls, a significant portion of the relaxation is an order of magnitude slower than in the bulk.

The orientational correlation time of a solute in a simple solvent is given by<sup>35</sup>

$$\tau = \frac{4\pi\eta r_H^3 f}{3k_B T} \quad (1)$$

where  $\eta$  is the solvent viscosity,  $r_H$  is the solute hydrodynamic radius,  $T$  is the temperature,  $k_B$  is Boltzmann's constant, and  $f$  is related to the boundary conditions for reorientation. OKE spectroscopy measures the collective orientational correlation time,  $\tau_c$ , of the solvent itself, but a graph of  $\tau_c$  versus  $\eta/T$  is generally linear for simple liquids.<sup>36</sup> Indeed,  $\tau_c$  behaves hydrodynamically over the

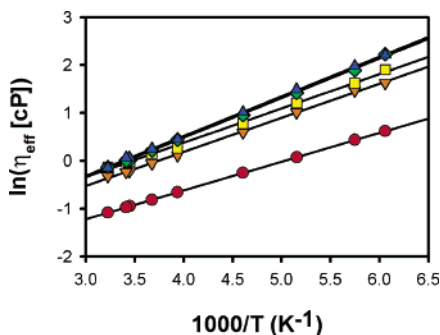


FIGURE 2. Arrhenius plots of the bulk viscosity (●) and effective surface viscosity of CS<sub>2</sub> in 45 (▼), 28 (■), 25 (◆), and 21 Å pores (▲).<sup>34</sup>

entire liquid temperature range of CS<sub>2</sub>.<sup>34</sup> The only parameters in eq 1 that might change near surfaces are  $\eta$ ,  $r_H$ , and  $f$ ; of these, only  $\eta$  should depend significantly on the temperature. Thus, if a change in  $\eta$  near the surfaces was alone responsible for the retardation of the molecular motion, an effective surface viscosity,  $\eta_{\text{eff}}$ , could be calculated from

$$\eta_{\text{eff}} = \frac{\langle \tau_{\text{surf}} \rangle}{\tau_{\text{bulk}}} \eta \quad (2)$$

where  $\langle \tau_{\text{surf}} \rangle$  is the average surface relaxation time (vide infra). The viscosity of CS<sub>2</sub> was measured at every temperature at which OKE measurements were made, and follows Arrhenius behavior.<sup>34</sup> As shown in Figure 2,  $\eta_{\text{eff}}$  also exhibits Arrhenius behavior, with a slope that is nearly identical to that of  $\eta$ . We interpret the fact that the activation energy for reorientation remains unchanged at the pore surfaces as indicating that it is not an increased viscosity that is responsible for the observed dynamic inhibition.

There is additional information to be gained from the amplitude of each exponential, which is proportional to the population of molecules that exhibit that orientational decay divided by the corresponding time constant. In other words, the signal,  $S(t)$ , is given by

$$S(t) \propto \frac{p_{\text{bulk}}}{\tau_{\text{bulk}}} e^{-t/\tau_{\text{bulk}}} + \frac{p_2}{\tau_2} e^{-t/\tau_2} + \frac{p_3}{\tau_3} e^{-t/\tau_3} \quad (3)$$

We can therefore determine the relative population corresponding to each time constant in the decay. We can further define an average surface relaxation time:

$$\langle \tau_{\text{surf}} \rangle = \frac{p_2 \tau_2 + p_3 \tau_3}{p_2 + p_3} \quad (4)$$

The corresponding surface population is given by

$$p_{\text{surf}} = p_2 + p_3 \quad (5)$$

Using  $p_{\text{surf}}$  and the pore radius, we can compute the thickness of the dynamically inhibited layer. Figure 3 shows how the thickness of the surface population of CS<sub>2</sub> depends on temperature. Notably, the dynamically inhibited

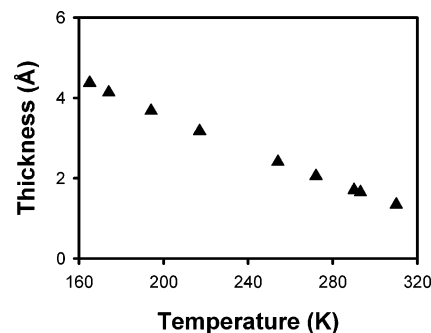


FIGURE 3. Estimated thickness of the dynamically inhibited surface layer of CS<sub>2</sub>.<sup>34</sup>

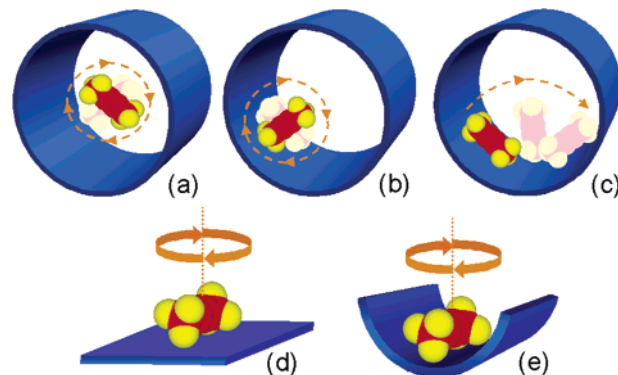


FIGURE 4. Schematic depiction of the hydrodynamic volume required for a 2-butyne molecule to reorient (a) far from a pore wall, (b) near a pore wall but pointing roughly along the surface normal, (c) off of a pore wall, (d) along a flat surface, and (e) along a curved surface.

surface population remains less than a monolayer thick over the entire liquid range of CS<sub>2</sub>.

Why is it that only a fraction of the molecules at the pore surfaces experience dynamic retardation? The answer to this question can be illustrated with another weakly wetting liquid we have studied, 2-butyne.<sup>37</sup> A molecule that is allowed to rotate freely will do so about its center of mass, as depicted in Figure 4a for a 2-butyne molecule near the center of a pore. Over the small angles required to restore the orientational isotropy of the liquid following the pump pulse, a molecule that is in contact with a surface and has its long axis perpendicular to the pore wall (Figure 4b) is also able to reorient about its center of mass. Such a molecule's hydrodynamic volume and rate of reorientation are identical to those in the bulk. However, if a molecule is in contact with the surface of a pore with its long axis parallel to the pore surface (Figure 4c), it cannot rotate off of the surface about its center of mass; it must instead pivot around one of its ends, increasing its hydrodynamic volume and thereby its orientational correlation time. The curvature of the pores additionally imposes a geometric boundary condition for the reorientation of molecules along the pore surfaces. Figure 4d depicts a 2-butyne molecule lying on a flat surface. This molecule can rotate about its center of mass in the plane that is parallel to the solid surface. However, if the surface is curved (Figure 4e), the molecule must move some distance away from the surface to reorient in this manner,



leading to dynamic inhibition. The degree of this inhibition increases as the pore radius decreases.

Room-temperature OKE scans were obtained for 2-butyne in the bulk and confined within 42, 62, and 91 Å diameter pores.<sup>37</sup> As was the case for CS<sub>2</sub>, the decay for bulk 2-butyne is fit well by a single exponential, whereas the decays for the confined liquid can be described by a sum of three exponentials. The fastest time constant in the confined OKE decays again matches that of the bulk and is assumed to arise from a bulklike population of molecules. The intermediate time constant is twice as large as  $\tau_{\text{bulk}}$ , regardless of the pore size, whereas the third time constant is approximately eight times larger than  $\tau_{\text{bulk}}$  and does depend on pore size.

For the purposes of interpreting these results, a molecule of 2-butyne can be modeled as a cylinder with a significant aspect ratio. The hydrodynamic volume required for the rotation of such a cylinder off of a surface would be expected to be twice that needed for reorientation about its center of mass. We therefore conclude that the intermediate exponential decay arises from reorientation off of the pore surfaces.<sup>37</sup> The fact that the value of this time constant is independent of pore size supports this assignment. On the other hand,  $\tau_3$  does increase modestly with decreasing pore diameter, which is consistent with dynamic inhibition due to geometric confinement effects.<sup>37</sup>

It is also interesting to contrast our results to those from studies of longer-time dynamics of supercooled weakly wetting liquids.<sup>18–20</sup> Because motions become considerably more cooperative as liquids are supercooled, the influence of the confining surfaces is felt over a significantly larger distance scale than in normal liquids, and the time scale for surface relaxation is therefore much slower than that in the bulk. However, it is still observed that the activation energy for surface reorientation is comparable to that of the bulk liquid.<sup>20</sup>

## Strongly Wetting Liquids

For some liquids, the presence of hydroxyl groups on the pore surfaces can lead to wetting via hydrogen bonding. In non-networked liquids, this hydrogen bonding can be comparable to or stronger than the attractive interactions among the liquid molecules themselves. Acetonitrile was studied as a prototypical liquid that does not exhibit strong networking but does accept hydrogen bonds from the surfaces. Temperature-dependent OKE data were collected in the bulk and in 24 and 42 Å pores.<sup>38,39</sup> Bulk acetonitrile exhibits exponential reorientational dynamics over its entire liquid temperature range, while the reorientation of the confined liquid can again be fit with a sum of three exponentials, the time constants of which are identical in both pore sizes.<sup>39</sup> The time constant of the fastest decay matches that of the bulk liquid, while the slowest reorientational time is approximately 20 times larger than that of the bulk liquid. Deuteration of the surface hydroxyl groups does not affect the OKE decays

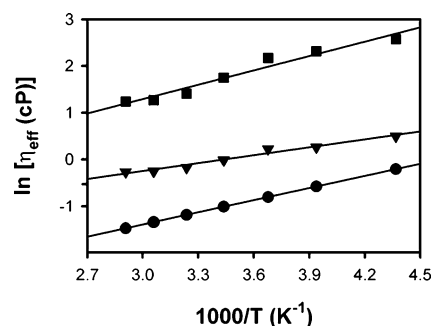


FIGURE 5. Arrhenius plot of  $\eta_{\text{eff}}$  for each exponential observed in the OKE decay of confined acetonitrile. Lines are linear least-squares fits to the data.<sup>39</sup>

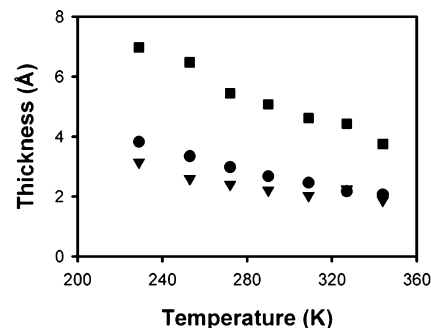
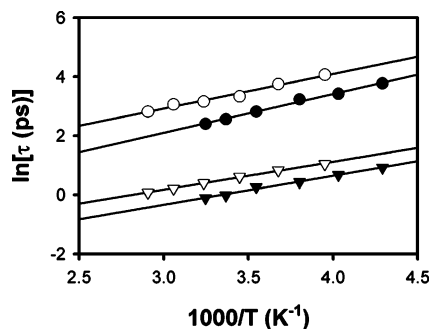


FIGURE 6. Temperature dependence of the estimated thickness of the surface layer of confined acetonitrile (■) and its breakdown into exchangeable (●) and nonexchangeable (▼) components.<sup>39</sup>

of the confined liquid, indicating that surface relaxation does not involve the breaking of hydrogen bonds.<sup>39</sup>

The effective viscosities associated with each exponential decay are plotted in Arrhenius form in Figure 5.<sup>38,39</sup> While the slopes for the fastest and slowest relaxation are similar (the corresponding activation energies are 7.2 kJ/mol and 8.5 kJ/mol, respectively), the slope for the intermediate relaxation is considerably smaller (the corresponding activation energy is 4.7 kJ/mol). The existence of a population with a lower activation energy for reorientation than in the bulk is not plausible, so we must look elsewhere to explain the origins of the decays.

We believe that the slowest relaxation arises from molecules bound to the pore surfaces. Since this relaxation is over 20 times slower than in the bulk, it is possible that exchange between the surface and bulklike populations can occur on a time scale faster than that of surface relaxation, opening a new channel for relaxation of surface molecules. To assess this idea, a kinetic model was developed<sup>39</sup> in which the surface population was divided into exchangeable and nonexchangeable portions, leading to a reorientational decay that is described well by a sum of three exponentials. The time constants and amplitudes of these exponentials can be used to calculate the relative populations and the rate constants of orientational relaxation. The temperature-dependent thickness of the surface layer and the thicknesses of the exchangeable and nonexchangeable portions of the surface layer as calculated from this model are shown in Figure 6. As expected, the thickness of the surface layer increases with decreasing temperature, and is greater than one monolayer at all



**FIGURE 7.** Arrhenius plots of the bulk (triangles) and surface (circles) orientational correlation times of acetonitrile from NMR (closed symbols) and OKE measurements (open symbols). Lines are linear least-squares fits to the data.<sup>39</sup>

temperatures. The exchangeable and nonexchangeable populations are similar in magnitude to one another at each temperature.

As an independent cross-check of our results, we compared them to Zhang and Jonas' NMR study of acetonitrile in sol–gel glasses.<sup>12</sup> The NMR time scale is much slower than that of reorientation, so NMR experiments provide a population-averaged single-molecule orientational correlation time,  $\tau_s$ . By using the surface-layer thickness derived from our data in conjunction with  $\tau_s$ , we can calculate the surface single-molecule orientational correlation time and compare it with the collective surface orientational correlation time that we measure. These times should be related by a factor that is weakly dependent on temperature and the magnitude of which depends on the degree of ordering in the liquid. Arrhenius plots of  $\tau_s$  and  $\tau_c$  in the bulk and at the pore surfaces are shown in Figure 7.<sup>39</sup> The plots for the bulk liquid are parallel, as are those for the surface relaxation, supporting our kinetic model. The larger separation between the plots of  $\tau_s$  and  $\tau_c$  at the pore surfaces indicates that, as expected, the liquid exhibits greater ordering there than in the bulk.

Finally, when acetonitrile is confined in pores in which the hydroxyl groups have been converted to hydrophobic groups, the orientational dynamics change drastically to resemble those of a weakly wetting liquid.<sup>39</sup> Two exponential decays are observed, one that matches that of the bulk liquid and one that is 3–4 times slower and depends on the pore size. Additionally, in hydrophobic pores the dynamically inhibited surface population is less than a monolayer thick over the full liquid temperature range of acetonitrile.

We can assemble this information into a coherent picture of the effects of confinement on acetonitrile.<sup>39</sup> The liquid in the pores separates into two populations, one of which is bulklike in behavior and the other of which has dynamics that are hindered by interactions with surface hydroxyl groups. There is also a possibility for exchange between the two populations, providing another pathway for orientational relaxation of the surface molecules. However, the relaxation of acetonitrile molecules that are hydrogen bonded to the surfaces does not involve breaking of hydrogen bonds, so these molecules cannot exchange. On the other hand, the sizable dipole moment of

acetonitrile (3.92 D)<sup>40</sup> presumably causes molecules to align in an antiparallel fashion at the pore surfaces, such that the unbound molecules that are interdigitated among the bound molecules are primed for exchange into the bulk. Support for this theory comes from the fact that the populations of exchangeable and nonexchangeable surface molecules are nearly equal.

## Networked Liquids

The existence of strong attractive intermolecular interactions can have a considerable influence on the behavior of a confined liquid, whether it wets the confining surfaces. Water is a case in point, and we have recently studied its dynamics at room temperature in both hydrophilic and hydrophobic pores.<sup>41</sup> There are significant differences between the behavior of water near hydrophilic and hydrophobic surfaces,<sup>42,43</sup> and how these differences are manifested in confinement is of importance, for instance, in many biological systems. At hydrophilic surfaces, the number of water–water hydrogen bonds decreases, as the water molecules tend to form hydrogen bonds with the surface,<sup>43</sup> thereby leading to significant dynamic inhibition. At hydrophobic surfaces, the dynamics of water are influenced by two competing effects. On one hand, the lack of hydrogen bonding to hydrophobic pore walls provides lubrication that augments the dynamics of the liquid.<sup>42,43</sup> On the other hand, since the water cannot hydrogen bond to the surface, additional hydrogen bonding occurs among the water molecules themselves, which tends to inhibit dynamics. Thus, the dynamics depend on a delicate balance of opposing effects that can be influenced by the pore size and the temperature, among other factors.

The OKE signal is proportional to the negative time derivative of the collective orientational correlation function,  $C_{\text{coll}}(t)$ .<sup>44</sup> We can therefore calculate this correlation function by integrating the OKE signal, so long as the constant of integration can be determined accurately.<sup>41</sup> If the OKE decay can be fit to a well-defined functional form, such as a sum of exponentials or a power law, this constant can be determined uniquely. An important advantage of calculating  $C_{\text{coll}}(t)$  is that the integration damps high-frequency noise, resulting in an improved signal-to-noise ratio at long delay times.

We have collected room-temperature OKE data for water confined to both hydrophilic and hydrophobic pores.<sup>41</sup> While water cannot enter dry hydrophobic glasses, it can displace another liquid that is filling the pores. Thus, glasses filled with CD<sub>3</sub>OH were soaked several times in water. The exchange of water for methanol within the pores was monitored by the disappearance of CD<sub>3</sub> vibrational modes in the IR spectrum. The glasses were subjected to a final water treatment after the CD<sub>3</sub> peak had disappeared from the IR absorption trace, at which point we estimate that at least 95% of the methanol had been removed.

The symmetry of a water molecule is such that water should exhibit a biexponential OKE decay.<sup>28</sup> We find that

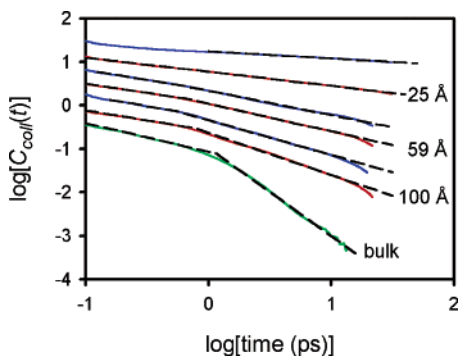


**FIGURE 8.** Log-log plots of  $C_{\text{coll}}(t)$  for water in the bulk and in confinement, along with power-law fits (dashed lines). The lower trace for each diameter is for hydrophilic pores and the upper trace is for hydrophobic pores. The data sets have been displaced for clarity.<sup>41</sup>

**Table 1. Fitting Parameters for  $C_{\text{coll}}(t)$ <sup>a</sup>**

sample	$\tau$ (ps)	$b_1$	$b_2$
bulk water	—	0.66	2.0
100 Å pores, unmodified	20	0.46	0.97
98 Å pores, modified	18	0.49	0.80
59 Å pores, unmodified	31	0.42	0.64
59 Å pores, modified	25	0.45	0.56
25 Å pores, unmodified	36		0.33
25 Å pores, modified	29		0.07

<sup>a</sup> Uncertainties in  $\tau$  are approximately  $\pm 2$  ps, and uncertainties in  $b_1$  and  $b_2$  are approximately  $\pm 0.03$ .

$C_{\text{coll}}(t)$  for bulk water can be fit reasonably well to a biexponential decay with time constants of 0.81 and 2.7 ps, in good agreement with the data of Winkler et al.<sup>45</sup> The slower decay arises from orientational relaxation, although the source of the faster decay is less certain. However, a close inspection of the residuals from this fit reveal systematic deviations, so we sought another way to analyze the data.<sup>41</sup> As shown in Figure 8, the bulk decay can be represented well by a pair of power laws,  $t^{-b}$ . The first power law has an exponent of  $b_1 = 0.66$  and is operative in the range of 100 fs to 1 ps. The second power law has an exponent of  $b_2 = 2.0$  and is observed from approximately 2 ps onward. We are working to derive a theoretical basis for power-law decays in water, but for our purposes here this should be taken only as a convenient empirical description.

Figure 8 also shows log–log plots of  $C_{\text{coll}}(t)$  for water confined in hydrophobic and hydrophilic pores having diameters of 25, 59, and 98 Å, along with power-law fits.<sup>41</sup> The power-law fits describe the confined water data well out to a time scale of approximately 15 ps, although in the smallest pores only a single power law is observed. At times longer than about 15 ps,  $C_{\text{coll}}(t)$  decays exponentially with a time constant that we will denote  $\tau$ . The values of  $b_1$ ,  $b_2$ , and  $\tau$  for each decay are listed in Table 1.

We believe that the long-time exponential decays observed in confinement arise from orientational relaxation at the pore surfaces. In all pore sizes, the surface relaxation is faster in hydrophobic pores than in hydrophilic pores, indicating that the lack of hydrogen bonding to the hydrophobic surfaces increases the rate of relaxation to a greater extent than it is decreased by the

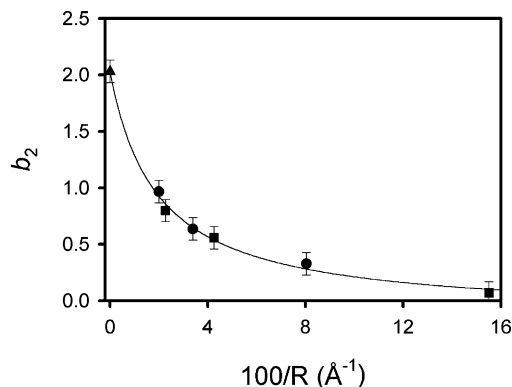


**FIGURE 9.** Variation of  $b_2$  with pore curvature for the bulk liquid (▲), hydrophilic pores (●), and hydrophobic pores (■). The radii of the hydrophobic pores have been decreased by 6 Å to account for surface modification. The line is a guide for the eye.<sup>41</sup>

additional hydrogen bonding among water molecules near the surfaces. This observation is in agreement with simulations of water at flat hydrophobic and hydrophilic surfaces.<sup>42,43</sup> Note, however, that the rate of surface relaxation does depend strongly on the pore diameter, suggesting that the relaxation is highly cooperative.

The second power law decay presumably arises from orientational relaxation of molecules that are not in contact with the pore walls. Strikingly, this relaxation shows no indication of bulklike dynamics in hydrophilic or hydrophobic pores of any size studied here. In all cases, the power-law exponent  $b_2$  is considerably smaller than the value of 2.0 observed in bulk water. Considering that the orientational dynamics are strongly perturbed even when the pore diameter is 98 Å, we conclude that the orientational relaxation of water involves cooperative motions that extend out to distance scales significantly larger than the diameter of a single molecule.

In contrast to the behavior of the long-time exponential relaxation, the values of  $b_2$  in Table 1 indicate that the relaxation of the molecules that are not in contact with the pore walls is slower in hydrophobic pores than in hydrophilic pores. However, it should be remembered that the process of making the pores hydrophobic also decreases the pore diameters. Indeed, as shown in Figure 9, if we assume that making the samples hydrophobic reduces the pore radius by 6 Å then  $b_2$  varies smoothly with pore curvature. Thus, while the dynamics of the liquid that is not in contact with the pore walls is highly cooperative in nature, it is not influenced substantially by the chemical nature of the pore surfaces.

## Conclusions

In this Account we have reviewed studies of the orientational dynamics of weakly wetting, strongly wetting, and networked liquids confined in nanoporous sol–gel glasses. OKE spectroscopy has allowed us to develop a detailed quantitative picture of the effects of confinement on the dynamics and structure of these liquids. In all the cases, the dynamics of the confined liquids are slower than those observed in the bulk. This inhibition arises from a number of different mechanisms, including geometrical con-



straints for reorientation at the pore surfaces and a change in the hydrodynamic volume for reorientation of molecules off of the pore walls in weakly wetting liquids, chemical interactions with functional groups on the pore surfaces in strongly wetting liquids, and interference with long-range cooperativity in networked liquids.

Liquids confined on the nanoscale exhibit a rich complexity of behavior, and the experiments described here have only begun to establish guiding principles for predicting how confinement will affect any given liquid. Many major avenues in this field that are of relevance to other areas of science and technology remain to be explored; for instance, little is known about how confinement affects the behavior of mixtures and solutions. Additionally, since OKE spectroscopy is sensitive primarily to orientational dynamics, it would be of great interest to perform complementary measurements of translational dynamics in the systems studied here, which can be accomplished for instance using pulsed-field-gradient spin–echo NMR spectroscopy<sup>46</sup> or quasi-elastic neutron scattering.<sup>47</sup> The dynamics of confined liquids will be a fertile and intriguing area of research for many years to come.

*This work was supported by the National Science Foundation, Grants CHE-9501598 and CHE-0073228. During portions of the period in which this work was completed, J.T.F. was a Dreyfus New Faculty Awardee, a Beckman Young Investigator, a Sloan Research Fellow, a Research Corporation Cottrell Scholar, and a Camille Dreyfus Teacher-Scholar. We thank Dr. Brian J. Loughnane, Dr. Alessandra Scodinu, and Thomas Reilly for their contributions to the research reviewed here.*

## References

- (1) In *Dynamics in Small Confining Systems III*; Drake, J. M., Klafter, J., Kopelman, R., Eds.; Materials Research Society: Pittsburgh, 1997; Vol. 464, p 388.
- (2) In *Dynamics in Small Confining Systems IV*; Drake, J. M., Grest, G. S., Klafter, J., Kopelman, R., Eds.; Materials Research Society: Warrendale, PA, 1999; Vol. 543, p 372.
- (3) Warnock, J.; Awschalom, D. D.; Shafer, M. W. Orientational Behavior of Molecular Liquids in Restricted Geometries. *Phys. Rev. B* **1986**, *34*, 475–478.
- (4) Brinker, C. J.; Scherer, G. W. *Sol-Gel Science: The Physics and Chemistry of Sol–Gel Processing*; Academic Press: San Diego, CA, 1990.
- (5) Righini, R. Ultrafast Optical Kerr Effect in Liquids and Solids. *Science* **1993**, *262*, 1386–1390.
- (6) Smith, N. A.; Meech, S. R. Optically-Heterodyne-Detected Optical Kerr Effect (OHD-OKE): Applications in Condensed Phase Dynamics. *Int. Rev. Phys. Chem.* **2002**, *21*, 75–100.
- (7) Nikiel, L.; Hopkins, B.; Zerda, T. W. Rotational and Vibrational Relaxation of Small Molecules in Porous Silica Gels. *J. Phys. Chem.* **1990**, *94*, 7458–7464.
- (8) Lee, Y. T.; Wallen, S. L.; Jonas, J. Effect of Confinement on the Resonant Intermolecular Vibrational Coupling of the  $\nu_2$  Mode of Methyl Iodide. *J. Phys. Chem.* **1992**, *96*, 7161–7164.
- (9) Wallen, S. L.; Nikiel, L.; Jonas, J. Confinement Effects on the Dynamics of Liquid Carbon Disulfide. *J. Phys. Chem.* **1995**, *99*, 15421–15427.
- (10) Liu, G.; Li, Y.-Z.; Jonas, J. Reorientational Dynamics of Molecular Liquids in Confined Geometries. *J. Chem. Phys.* **1989**, *90*, 5881–5882.
- (11) Liu, G.; Li, Y.; Jonas, J. Confined Geometry Effects on Reorientational Dynamics of Molecular Liquids in Porous Silica Glasses. *J. Chem. Phys.* **1991**, *95*, 6892–6901.
- (12) Zhang, J.; Jonas, J. NMR Study of the Geometric Confinement Effects of the Anisotropic Rotational Diffusion of Acetonitrile- $d_3$ . *J. Phys. Chem.* **1993**, *97*, 8812–8815.
- (13) Xu, S.; Jonas, J. <sup>13</sup>C NMR Relaxation Studies of Pyridine and Pentafluoropyridine Liquids Confined to Nanopores of Porous Silica Glasses. *J. Phys. Chem.* **1996**, *100*, 16242–16246.
- (14) Korb, J.-P.; Xu, S.; Cros, F.; Malier, L.; Jonas, J. Quenched Molecular Reorientation and Angular Momentum for Liquids Confined to Nanopores of Silica Glass. *J. Chem. Phys.* **1997**, *107*, 4044–4050.
- (15) Carini, G.; Crupi, V.; D'Angelo, G.; Majolino, D.; Migliardo, P.; Mel'nichenko, Y. B. Relaxation Dynamics of H-Bonded Liquids Confined in Porous Silica Gels by Rayleigh Wing Spectroscopy. *J. Chem. Phys.* **1997**, *107*, 2292–2299.
- (16) Crupi, V.; Majolino, D.; Migliardo, P.; Venuti, V. Diffusive Relaxations and Vibrational Properties of Water and H-Bonded Systems in Confined State by Neutrons and Light Scattering: State of the Art. *J. Phys. Chem. A* **2000**, *104*, 11000–11012.
- (17) Crupi, V.; Dianoux, A. J.; Majolino, D.; Migliardo, P.; Venuti, V. Dynamical Response of Liquid Water in Confined Geometry by Laser and Neutron Spectroscopies. *Phys. Chem. Chem. Phys.* **2002**, *4*, 2768–2773.
- (18) Mel'nichenko, Y. B.; Schuller, J.; Richert, R.; Ewen, B.; Loong, C.-K. Dynamics of Hydrogen-Bonded Liquids Confined to Mesopores: A Dielectric and Neutron Spectroscopy Study. *J. Chem. Phys.* **1995**, *103*, 2016–2024.
- (19) Richert, R. Geometrical Confinement and Cooperativity in Supercooled Liquids Studied by Solvation Dynamics. *Phys. Rev. B* **1996**, *54*, 15762–15766.
- (20) Yang, M.; Richert, R. Surface Induced Glass Transition in a Confined Molecular Liquid. *J. Phys. Chem. B* **2003**, *107*, 895–898.
- (21) Baumann, R.; Ferrante, C.; Deeg, F. W.; Brauchle, C. Solvation Dynamics of Nile Blue in Ethanol Confined in Porous Sol-Gel Glasses. *J. Chem. Phys.* **2001**, *114*, 5781–5791.
- (22) Arndt, M.; Stannarius, R.; Gorbatschow, W.; Kremer, F. Dielectric Investigations of the Dynamic Glass Transition in Nanopores. *Phys. Rev. E* **1996**, *54*, 5377–5390.
- (23) Arndt, M.; Stannarius, R.; Grootthues, H.; Hempel, E.; Kremer, F. Length Scale of Cooperativity in the Dynamic Glass Transition. *Phys. Rev. Lett.* **1997**, *79*, 2077–2080.
- (24) Huwe, A.; Arndt, M.; Kremer, F.; Haggemuller, C.; Behrens, P. Dielectric Investigation of the Molecular Dynamics of Propanediol in Mesoporous Silica Materials. *J. Chem. Phys.* **1997**, *107*, 9699–9701.
- (25) Pissis, P.; Daoukaki, D.; Apekis, L.; Christodoulides, C. The Glass Transition in Confined Liquids. *J. Phys.: Condens. Matter* **1994**, *6*, L325–L328.
- (26) Pissis, P.; Kyritsis, A.; Daoukaki, D.; Barut, G.; Pelster, R.; Nimtz, G. Dielectric Studies of Glass Transition in Confined Polypropylene Glycol. *J. Phys.: Condens. Matter* **1998**, *10*, 6205–6227.
- (27) Iler, R. K. *The Chemistry of Silica*; Wiley: New York, 1979.
- (28) Berne, B. J.; Pecora, R. *Dynamic Light Scattering*; Wiley: New York, 1976.
- (29) Kivelson, D.; Madden, P. A. Light Scattering Studies of Molecular Liquids. *Annu. Rev. Phys. Chem.* **1980**, *31*, 523–558.
- (30) Loughnane, B. J.; Farrer, R. A.; Scodinu, A.; Reilly, T.; Fourkas, J. T. Ultrafast Spectroscopic Studies of the Dynamics of Liquids Confined in Nanoporous Glasses. *J. Phys. Chem. B* **2000**, *104*, 5421–5429.
- (31) McMorrow, D.; Lotshaw, W. T. Intermolecular Dynamics in Acetonitrile Probed with Femtosecond Fourier Transform Raman Spectroscopy. *J. Phys. Chem.* **1991**, *95*, 10395–10406.
- (32) Loughnane, B. J.; Fourkas, J. T. Geometric Effects in the Dynamics of a Nonwetting Liquid in Microconfinement: An Optical Kerr Effect Study of Methyl Iodide in Nanoporous Glasses. *J. Phys. Chem. B* **1998**, *102*, 10288–10294.
- (33) Farrer, R. A.; Loughnane, B. J.; Fourkas, J. T. Dynamics of Confined Carbon Disulfide from 165 to 310 K. *J. Phys. Chem. A* **1997**, *101*, 4005–4010.
- (34) Loughnane, B. J.; Scodinu, A.; Fourkas, J. T. Extremely Slow Dynamics of a Weakly Wetting Liquid at a Solid/Liquid Interface: CS<sub>2</sub> Confined in Nanoporous Glasses. *J. Phys. Chem. B* **1999**, *103*, 6061–6068.
- (35) Debye, P. *Polar Molecules*; Dover: New York, 1929.
- (36) Loughnane, B. J.; Scodinu, A.; Farrer, R. A.; Fourkas, J. T. Exponential Intermolecular Dynamics in Optical Kerr Effect Spectroscopy of Small-Molecule Liquids. *J. Chem. Phys.* **1999**, *111*, 2686–2694.
- (37) Scodinu, A.; Farrer, R. A.; Fourkas, J. T. Direct Observation of Different Mechanisms for the Inhibition of Molecular Reorientation at a Solid/Liquid Interface. *J. Phys. Chem. B* **2002**, *106*, 12863–12865.
- (38) Loughnane, B. J.; Farrer, R. A.; Fourkas, J. T. Evidence for the Direct Observation of Molecular Exchange of a Liquid at the Solid/Liquid Interface. *J. Phys. Chem. B* **1998**, *102*, 5409–5412.

- (39) Loughnane, B. J.; Farrer, R. A.; Scodinu, A.; Fourkas, J. T. Dynamics of a Wetting Liquid in Nanopores: An Optical Kerr Effect Study of the Dynamics of Acetonitrile Confined in Sol-Gel Glasses. *J. Chem. Phys.* **1999**, *111*, 5116–5123.
- (40) Weast, R. C. *CRC Handbook of Chemistry and Physics*, 66th ed.; CRC Press: Boca Raton, FL, 1985.
- (41) Scodinu, A.; Fourkas, J. T. Comparison of the Orientational Dynamics of Water Confined in Hydrophobic and Hydrophilic Nanopores. *J. Phys. Chem. B* **2002**, *106*, 10292–10295.
- (42) Lee, C. Y.; McCammon, J. A.; Rosky, P. J. The Structure of Liquid Water at an Extended Hydrophobic Surface. *J. Chem. Phys.* **1984**, *80*, 4448–4455.
- (43) Lee, S. H.; Rosky, P. J. A Comparison of the Structure and Dynamics of Liquid Water at Hydrophobic and Hydrophilic Surfaces—A Molecular Dynamics Simulation Study. *J. Chem. Phys.* **1994**, *100*, 3334–3345.
- (44) Dhar, L.; Rogers, J. A.; Nelson, K. A. Time-Resolved Vibrational Spectroscopy in the Impulsive Limit. *Chem. Rev.* **1994**, *94*, 157–193.
- (45) Winkler, K.; Lindner, J.; Bursing, H.; Vohringer, P. Ultrafast Raman-Induced Kerr-Effect of Water: Single Molecule Versus Collective Motions. *J. Chem. Phys.* **2000**, *113*, 4674–4682.
- (46) Price, W. S. Pulsed-Field Gradient Nuclear Magnetic Resonance as a Tool for Studying Translational Diffusion: Part II. Experimental Aspects. *Concepts Magn. Reson.* **1998**, *10*, 197–237.
- (47) Trouw, F. R.; Price, D. L. Chemical Applications of Neutron Scattering. *Annu. Rev. Phys. Chem.* **1999**, *50*, 571–601.

AR0200302